iScience

CellPress
OPEN ACCESS

Article

Obg-like ATPase 1 exacerbated gemcitabine drug resistance of pancreatic cancer

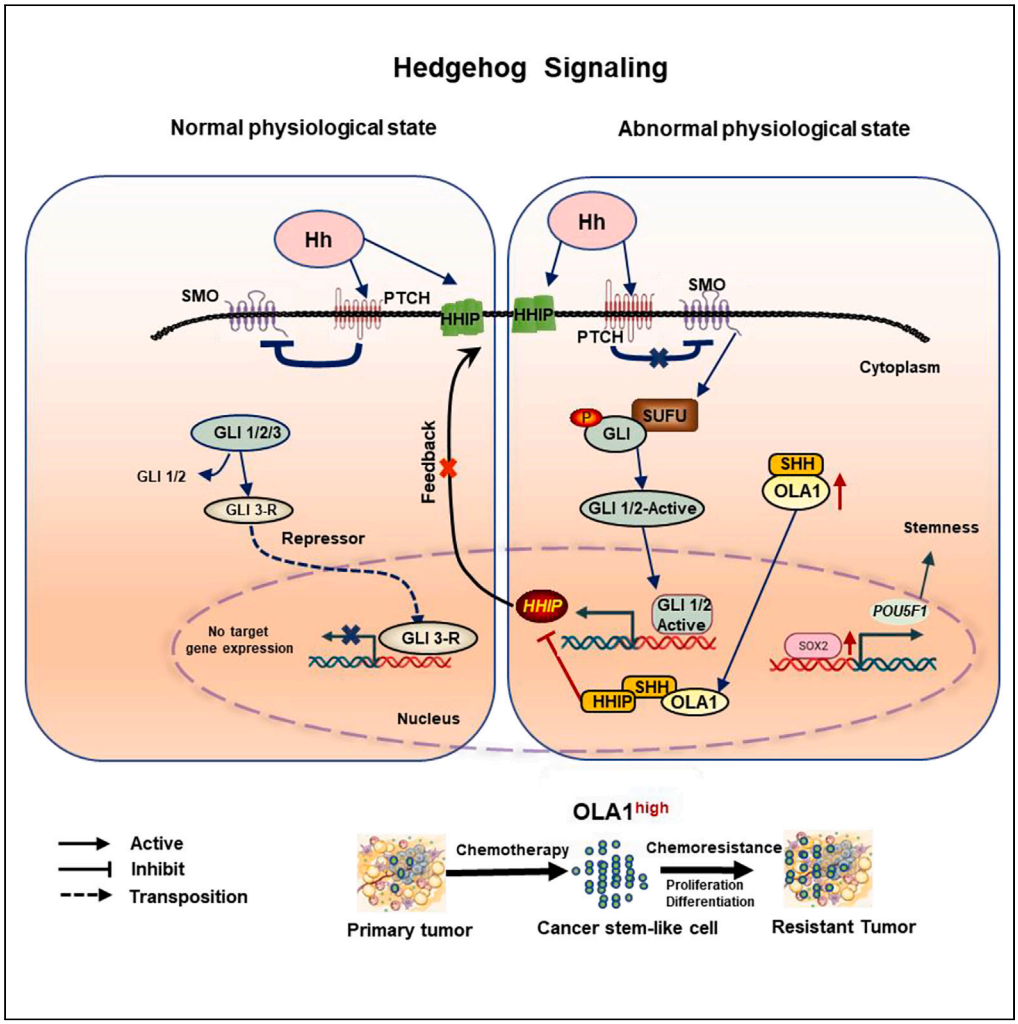

Jianzhou Liu, Jing Huang, Jun Lu, ..., Vay Liang W(Bill) Go, Junchao Guo, Gary Guishan Xiao

gjcpumch@163.com (J.G.)
gxiao@dlut.edu.cn (G.G.X.)

Highlights

OLA1 promotes PDAC chemoresistance by enhancing CSC characteristics

OLA1 binds directly to SHH to regulate the hedgehog pathway

OLA1 reduced GEM sensitivity in PDAC cells by co-activation with SHH/HHIP cascades

Liu et al., iScience 27, 110027
June 21, 2024
https://doi.org/10.1016/j.isci.2024.110027

iScience

CellPress
OPEN ACCESS

Article

Obg-like ATPase 1 exacerbated gemcitabine drug resistance of pancreatic cancer

Jianzhou Liu,[1,2,3] Jing Huang,[2] Jun Lu,[4] Runze Ouyang,[5] Wenchao Xu,[1] Jianlu Zhang,[1] Kevin Chen-Xiao,[6] Chengjun Wu,[7] Dong Shang,[8] Vay Liang W(Bill) Go,[9] Junchao Guo,[1,11,*] and Gary Guishan Xiao[2,9,10,*]

SUMMARY

Pancreatic ductal adenocarcinoma (PDAC) is a highly malignant disease with a poor prognosis due to inefficient diagnosis and tenacious drug resistance. Obg-like ATPase 1 (OLA1) is overexpressed in many malignant tumors. The molecular mechanism of OLA1 underlying gemcitabine (GEM)-induced drug resistance was investigated in this study. An enhanced expression of OLA1 was observed in a GEM acquired resistant pancreatic cancer cell lines and in patients with pancreatic cancer. Overexpressed OLA1 showed poor overall survival rates in patients with pancreatic cancer. Dysregulation of the OLA1 reduced expression of $CD44^{+}$/CD133+, and improved the sensitivity of pancreatic cancer cells to GEM. OLA1 highly expression facilitated the formation of the OLA1/Sonic Hedgehog (SHH)/Hedgehog-interacting protein (HHIP) complex in nuclei, resulting in the inhibition of negative feedback of Hedgehog signaling induced by HHIP. This study suggests that OLA1 may be developed as an innovative drug target for an effective therapy of pancreatic cancer.

INTRODUCTION

Pancreatic ductal adenocarcinoma (PDAC) is a poor prognostic disease with 5-year survival rate of only about 10%,[1–4] largely because of its inefficient diagnosis and tenacious drug resistance.[5] Pancreatic cancer relapse during therapy remains major challenges for improving overall cancer survival that may be still due partially to the existence of cancer stem cells (CSCs). A line of study shows that cancer cells during the course of therapy may be in part transformed into cancer stem-like cells (CSCs) in response to the treatment.[6,7] CSCs are characterized by tumorigenic and self-renewal properties and the ability to produce differentiated progeny, resulting in tumor recurrence, invasion, and metastasis, and causing resistance to therapy. Pancreatic CSCs, first identified by Li et al. in 2007, are heavily associated with drug resistance in patients with PDAC treated with conventional therapeutic regimens, and with metastasis and recurrence.[8,9] Targeting CSCs thus becomes an essential strategy for reducing drug resistance of tumor cells and suppressing tumor metastasis and relapse.[10] However, despite the central role of these CSCs playing in cancer progression, the regulation of their key features, such as stemness and tumorigenicity, remains still incompletely understood.

Obg-like ATPase 1 (OLA1) is a P loop GTPase belonging to the translation factor-related (TRAFAC) class, the Obg family, and the YchF subgroup. TRAFAC GTPases include translation factors and ribosomal connexin, signal transduction, intracellular transport, and stress-response proteins.[11,12] OLA1 is highly conserved from bacteria to humans and, unlike other Obg family members, possesses both GTPase and ATPase activities.[13,14] OLA1 has been reported to be highly expressed in a variety of tumors[15] and to be involved in regulating many critical cellular activities,[16,17] including tumorigenesis,[18] cell proliferation,[15] DNA damage repair,[19] centrosome regulation,[20–22] the Warburg effect,[23] mitochondrial bioenergetic function[24] and prognosis.[25,26] In addition, OLA1 can also sense changes in the external environment, such as temperature changes,[27,28] nutrient deficiency,[29] and drug stimulation, and affect the cellular stress response[17,30,31] and drug sensitivity.[32] OLA1 is also involved in the epithelial–mesenchymal transition (EMT) in various tumor cells.[33,34] One report showed that EMT was not required for metastasis, but may contribute to chemoresistance.[35] However, the molecular mechanism underlying OLA1-mediated

[1]Department of General Surgery, State Key Laboratory of Complex Severe and Rare Diseases, Peking Union Medical College Hospital, Chinese Academy of Medical Sciences and Peking Union Medical College, Beijing 100730, China
[2]State Key Laboratory of Fine Chemicals, Department of Pharmaceutical Sciences, School of Chemical Engineering, Dalian University of Technology, Dalian 116024, China
[3]Institute of clinical medicine, Peking Union Medical College Hospital, Chinese Academy of Medical Sciences and Peking Union Medical College, Beijing 100730, China
[4]Department of General Surgery, Peking University Third Hospital, Beijing 100191, China
[5]CAS Key Laboratory of Separation Science for Analytical Chemistry, Dalian Institute of Chemical Physics, Chinese Academy of Sciences, Dalian, China
[6]Department of Nutritional Sciences and Toxicology, University of California Berkeley, San Francisco, CA, USA
[7]School of Biomedical Engineering, Dalian University of Technology, Dalian, China
[8]Department of General Surgery, Clinical Laboratory of Integrative Medicine, The First Affiliated Hospital of Dalian Medical University, Dalian 116011, Liaoning, China
[9]The UCLA Agi Hirshberg Center for Pancreatic Diseases, David Geffen School of Medicine at UCLA, Los Angeles, CA, USA
[10]Functional Genomics and Proteomics Laboratory, Osteoporosis Research Center, Creighton University Medical Center, Omaha, NE, USA
[11]Lead contact
*Correspondence: gjcpumch@163.com (J.G.), gxiao@dlut.edu.cn (G.G.X.)
https://doi.org/10.1016/j.isci.2024.110027

processes in drug-resistant cells in pancreatic cancer is unclear. This study showed that OLA1 induced chemoresistance in pancreatic cancer resulting from its co-activation of Sonic hedgehog (SHH)/Hedgehog-interacting protein (HHIP) cascades.

RESULTS

Correlation of Obg-like ATPase 1 *expression* with chemoresistance in cells and tissues of pancreatic ductal adenocarcinoma

Analysis of the Cancer Genome Atlas (TCGA) normal and Genotype-Tissue Expression (GTEx) in Gene Expression Profiling Interactive Analysis (GEPIA) databases was performed to understand the role of OLA1 in chemoresistance. *OLA1* was significantly upregulated in basal ($N = 65$) and classical ($N = 86$) pancreatic cancers compared with paired normal tissues ($N = 171$) (Figure S1A). A meta-analysis of OLA1 expression in patients with pancreatic cancer showed that *OLA1* was negatively correlated with overall survival (OS) and disease-free survival (DFS) in these patients (Figures S1B and S1C). Investigating the correlation between drug treatment sensitivity and OLA1 expression in patients with pancreatic cancer, we conducted a comprehensive analysis of clinical data from 94 individuals who received standardized chemotherapy, within a cohort of 265 patients undergoing surgical resection for pancreatic cancer. Utilizing clinicians' assessments of treatment responses, chemotherapy outcomes were classified as either "sensitive" or "tolerant." We determined if endogenous levels of OLA1 in pancreatic cancer tissues were associated with drug responsiveness by immunohistochemistry (IHC) analysis of pancreatic cancer tissues from patients with differential drug responsiveness, and showed higher levels of OLA1 in pancreatic cancer tissues compared with para-cancerous tissues ($p < 0.001$) (Figure 1A). Moreover, elevated FAK expression was notably associated with a shortened cancer-specific survival ($p = 0.0243$, Figure 1B). Notably, endogenous OLA1 expression exhibited significant associations with gender ($p = 0.046$), pathological M stage ($p = 0.012$), chemotherapy responses ($p = 0.04$), and clinical stage ($p = 0.039$), as detailed in Table 1. Noteworthy, patients deemed chemotherapy-sensitive exhibited prolonged survival (Figure 1C). Interestingly, within different chemotherapy regimens, heightened OLA1 expression correlated with diminished efficacy of gemcitabine (GEM) chemotherapy (Figure 1D). However, due to the limited number of enrolled cases in other chemotherapy regimens, statistical distinctions were challenging to observe. We explored the association between OLA1 expression and GEM resistance in pancreatic cancer by comparing OLA1 expression levels in tissues obtained from GEM-tolerant and GEM-sensitive patients. Our analysis revealed a significant elevation in OLA1 expression among GEM-tolerant patients. (Figures 1E and 1F). We verified these findings by comparing OLA1 mRNA and protein levels in seven pancreatic cancer cell lines (CFPAC-1, AsPC-1, MIA-PaCa-2, BxPC-3, SW1990, HPAF-II, and PANC-1) with normal human pancreatic ductal epithelial cells (HPDE6-C7), and showed that endogenous levels of OLA1 were higher in intrinsic GEM-resistant cells, such as PANC-1 and HPAF-II cells, compared with GEM-sensitive cell lines (Figures 1G and 1H). *OLA1* was induced in SW1990 cells exposed to serial GEM concentrations (Figures 1I and 1J). We determined if endogenous OLA1 was related to drug resistance during long-term GEM exposure by creating a GEM-acquired-resistance BxPC-3 cell line (BxGR) (Figure 1K). We then analyzed endogenous OLA1 mRNA (Figure 1L) and protein levels (Figure 1M) in the GEM-resistant BxGR cells. Endogenous levels of OLA1 mRNA and protein were significantly higher in GEM-resistant cells than in the parental cells. To systematically delineate changes in the expression of drug-resistance related genes, transcriptomic sequencing was conducted on the BxGR-10 cell line (Figure 1N). Enrichment analysis of molecular functions revealed significant disparities, particularly in GTP binding and GTPase activity (Figure 1O). Additionally, we conducted statistical analyses on the expression of genes associated with ABC transporters and GEM resistance. Notably, the drug-resistant cell line BxGR-10 exhibited the heightened expression of cytidine deaminase (CDA) and OLA1, consistent with previous reports on the elevated expression of CDA in GEM-resistant pancreatic cancer cell lines. Furthermore, we observed the elevated expression of several ABC transporter family genes, including ABCA3, ABCG2, ABCC4, ABCB9, ABCD1, and ABCC1 (Figure 1P), suggesting their potential involvement in the transport of GEM substrates. These results indicated a potential regulatory role for OLA1 in the development of drug resistance in pancreatic tumors.

Knockdown of Obg-like ATPase 1 enhanced chemosensitivity

To clarify the regulatory role of OLA1 in the development of drug resistance, we transfected PANC-1, BxPC-3, and SW1990 cells with *OLA1* small interfering RNA (siOLA1), short hairpin silencing RNA (LV3-shOLA1), and OLA1 transient (pdEYFP-N1gen-OLA1) or inducible transfection (pLV-TRE-OLA1) plasmids (Figures 2A–2C, S2A, and S2B). GEM sensitivity of pancreatic cancer cells was recovered while OLA1 knocked down (Figures 2D–2G). Intriguingly, pancreatic cancer cells with *OLA1* overexpression treated with other drugs, such as paclitaxel (PTX), showed a similar response to GEM (Figures 2H–2J). Although silencing OLA1 did not exert a discernible impact on the expression of the GEM-resistance genes RRM1 and CDA, it did induce alterations in the expression of other drug-resistance genes. Specifically, changes were observed in the expression of ABCB1, ABCG1, ABCC1, ABCC2, and ABCA3, as evidenced by BxGR RNA-sequencing data (Figure 2K). To further explore the regulatory effect of OLA1 on GEM chemoresistance of pancreatic cancer, RNA-sequencing (RNA-seq) was performed in stably OLA1 knocked-down SW1990 cells (Figures S3A and S3B). Moreover, upon analyzing the transcriptomic sequencing results of OLA1 knockout cells, we observed differential expression among the ABC transporter families. Notably, among these, only ABCC1 overlapped with the sequenced ABC transporter family identified in the constructed BxGR cell lines (Figure 2L). Cytological results suggested that the mechanism underlying OLA1-mediated GEM resistance may differ from the classical mechanism for pyrimidine nucleoside synthesis. We therefore examined the role of OLA1 in GEM resistance *in vivo* using a Tet-on system with doxycycline-inducible *OLA1* overexpression ($OLA1^{iOE}$) (Figure 2M). Subcutaneous xenograft tumors were established in Balb/c nude mice, as shown in the flowchart (Figure 2N). Bodyweights of mice in the vector GEM group were lower than in the other three groups (Figure 2O). As OLA1 was induced, mice in the $OLA1^{iOE}$ group showed GEM resistance (Figure 2P), in which both the tumor volume (Figure 2Q) and the tumor weight (Figure 2R) were significantly increased. To further understand the effect of OLA1 on GEM resistance in SW1990 cells, mice in the $OLA1^{iOE}$ and the control group were treated either GEM or saline, respectively. The results showed that the ratio of the tumor weight in mice treated with GEM to that in control was significantly

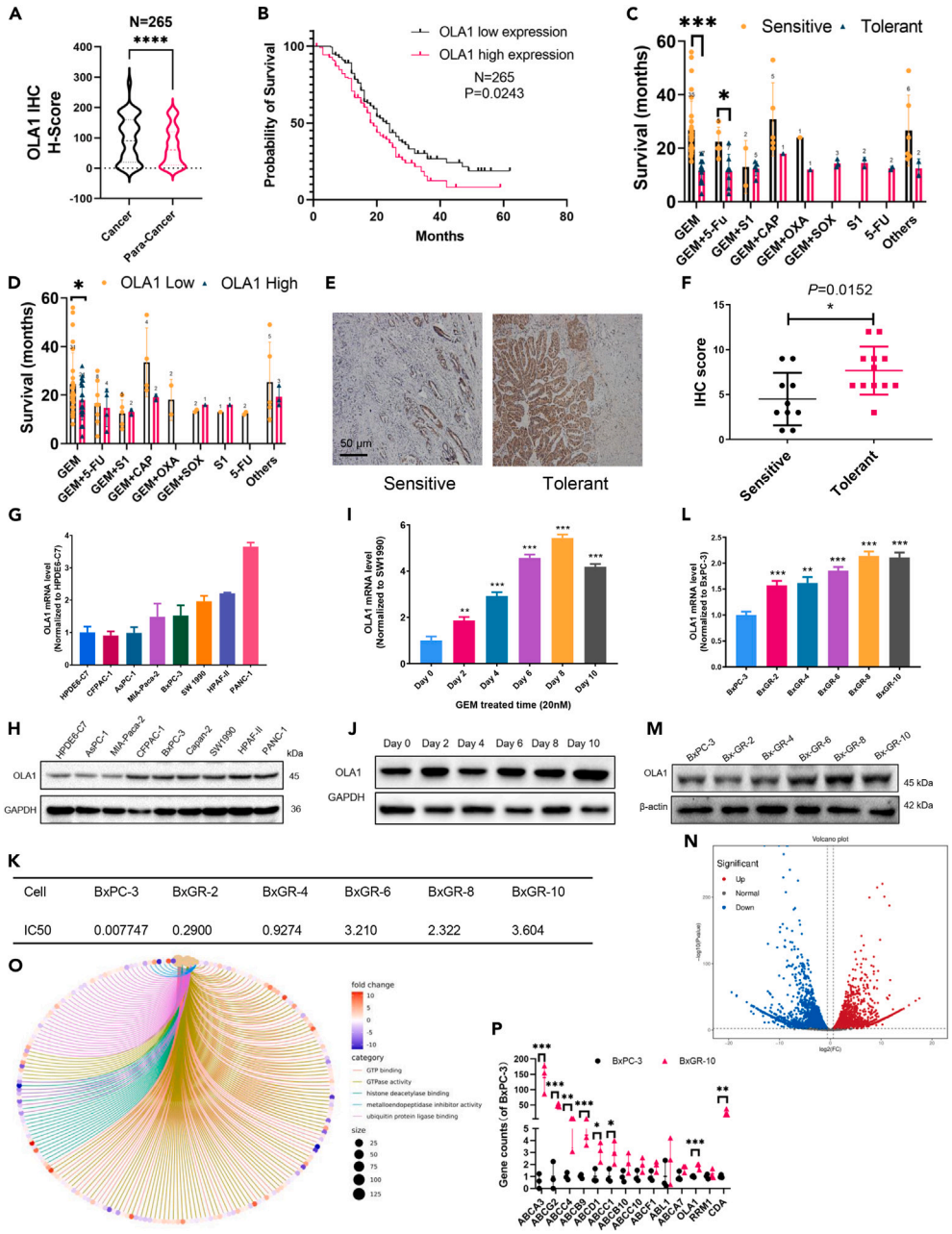

Figure 1. Correlation of OLA1 expression with chemoresistance in cells and tissues of in PDAC

(A) Tissue microarrays were utilized to assess OLA1 protein expression levels in 265 patients with pancreatic cancer.

(B) Patients exhibiting high tumoral OLA1 expression demonstrated significantly poorer cancer-specific survival compared to those with low OLA1 expression.

(C) The impact of sensitivity to different chemotherapy regimens on survival.

(D) The effect of OLA1 expression on the survival of patients undergoing different chemotherapy regimens.

(E) Tumor tissues were obtained from patients categorized as either drug-sensitive or drug-resistant based on the efficacy of GEM chemotherapy. Scale bars of 50 μm were included for reference.

(F) OLA1 IHC score was detected by immunohistochemistry.

(G) *OLA1* mRNA expression in a human pancreatic ductal epithelial cell line (HPDE6-C7) and seven pancreatic cancer cell lines.

(H) OLA1 expression in a human pancreatic ductal epithelial cell line (HPDE6-C7) and eight pancreatic cancer cell lines. OLA1 mRNA (I) and protein (J) expression in cells with short-term GEM exposure.

(K) IC50 in BxPC-3 GEM-resistant cells after long-term GEM exposure. OLA1 mRNA (L) and protein (M) expression in BxPC-3 and BxGR (BxPC-3 GEM resistance) cells.

(N) Transcriptomically sequenced gene expression volcano map of acquired drug-resistant cells (O) Molecular functional annotation of acquired drug resistant cells.

(P) mRNA expression of ABC transporter protein family changes in acquired drug resistant cells *$p < 0.05$; **$p < 0.01$; ***$p < 0.001$.

Table 1. Correlations between OLA1 expression and clinicopathological features of PDAC

		Cytoplasmic OLA1 expression		
Variable	n	Low	High	*p*-value
Patients	265	138	127	–
Age (years)				0.324
≤60	121	67	54	
>60	144	70	74	
Gender				0.046*
Male	154	88	66	
Female	111	49	62	
Tumor location				0.130
Head	147	82	65	
Non-head	110	50	60	
CA19-9 (U/ml)				0.507
≤34	45	20	25	
>34	183	93	90	
Histologic grade				0.339
G1-2	146	76	70	
G3-4	86	51	35	
pT stage				0.639
T1-2	19	11	8	
T3-4	246	126	120	
pN stage				0.902
N0	118	62	56	
N1-2	147	75	72	
pM stage				0.033*
M0	219	123	96	
M1	15	4	11	
Margin				0.534
R0	162	85	77	
R1	27	12	15	
Chemotherapy Response				0.040*
Sensitive	54	39	15	
Tolerant	40	21	19	
Clinical stage				0.039*
I, II	244	131	113	
III, IV	21	6	15	

Partial data were not available, and statistical analyses were based on available data.
p-values were derived from the $\chi 2$ test (two-sided).
G1, well differentiated; G2, moderately differentiated; G3, poorly differentiated; pT stage, pathological T stage; pN stage, pathological N stage; pM stage, pathological M stage.
*$p < 0.05$.
†Fisher's exact test (two-sided) was used when the expected values in 20% or more of the cells of a contingency table were below 5.

enhanced (Figure 2S), while the Ki67 level in the OLA1^{iOE} group was also significantly increased as compared to control, which was further verified by H&E stain (Figure 2T). All together, it is suggested that OLA1 may play a role in GEM-induced chemoresistance of PDAC cells.

Obg-like ATPase 1 induced cancer stem cell characteristics

CSCs play a pivotal role in tumor drug resistance. Analysis of transcriptomic sequencing data from the acquired resistant cell line BxGR revealed a significant association between OLA1 and stemness biomarkers. Specifically, the Yamanaka factors POU5F1 and SOX2 exhibited

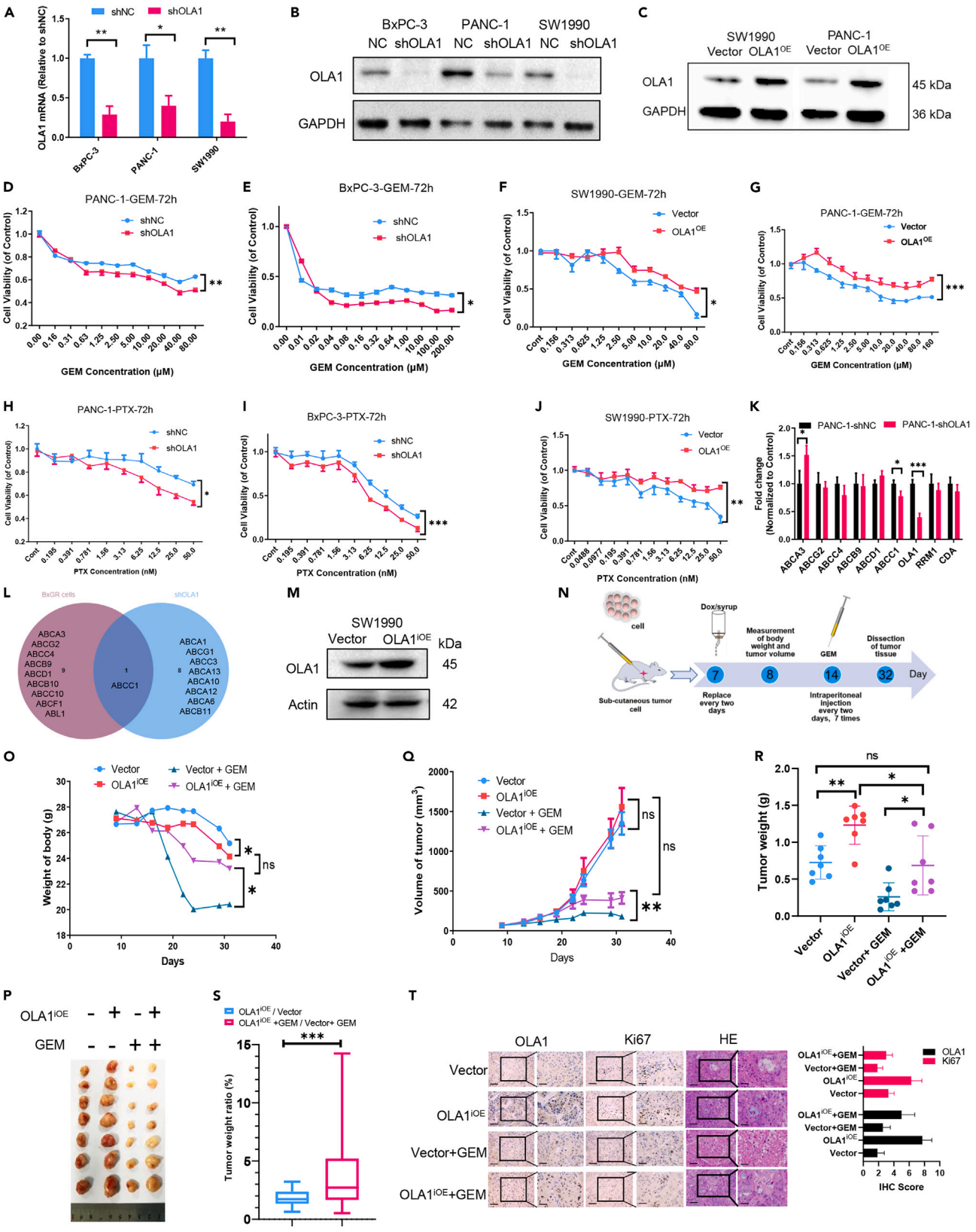
A
shNC
shOLA1
OLA1 mRNA (Relative to shNC)
BxPC-3
PANC-1
SW1990
B
BxPC-3 PANC-1 SW1990
NC shOLA1 NC shOLA1 NC shOLA1
OLA1
GAPDH
C
SW1990 PANC-1
Vector OLA1OE Vector OLA1OE
OLA1
GAPDH
45 kDa
36 kDa
D
PANC-1-GEM-72h
shNC
shOLA1
Cell Viability (of Control)
GEM Concentration (μM)
E
BxPC-3-GEM-72h
F
SW1990-GEM-72h
Vector
OLA1OE
G
PANC-1-GEM-72h
H
PANC-1-PTX-72h
PTX Concentration (nM)
I
BxPC-3-PTX-72h
J
SW1990-PTX-72h
K
PANC-1-shNC
PANC-1-shOLA1
Fold change (Normalized to Control)
ABCA3
ABCG2
ABCC4
ABCB9
ABCD1
ABCC1
OLA1
RRM1
CDA
L
BxGR cells
shOLA1
ABCA3
ABCG2
ABCC4
ABCB9
ABCD1
ABCB10
ABCC10
ABCF1
ABL1
ABCC1
ABCA1
ABCG1
ABCC3
ABCA13
ABCA10
ABCA12
ABCA6
ABCB11
M
SW1990
Vector OLA1iOE
kDa
OLA1
Actin
45
42
N
cell
Dox/syrup
Measurement of body weight and tumor volume
GEM
Dissection of tumor tissue
Sub-cutaneous tumor cell
Replace every two days
Intraperitoneal injection every two days, 7 times
Day
O
Vector
OLA1iOE
Vector + GEM
OLA1iOE + GEM
Weight of body (g)
Days
Q
Volume of tumor (mm3)
ns
R
Tumor weight (g)
Vector
OLA1iOE
Vector+ GEM
OLA1iOE +GEM
P
OLA1iOE
GEM
S
OLA1iOE / Vector
OLA1iOE +GEM / Vector+ GEM
Tumor weight ratio (%)
T
OLA1
Ki67
HE
Vector
OLA1iOE
Vector+GEM
OLA1iOE+GEM
IHC Score

Figure 2. Knockdown of *OLA1* enhanced chemosensitivity

OLA1 mRNA (A) and protein (B) expression in cells with stable knockdown of *OLA1*.

(C) Western blot of OLA1 protein in SW1990 and PANC-1 OLA1^{OE} cells. Viability of PANC-1 (D) and BxPC-3 (E) cells with *OLA1* knockdown after GEM treatment for 72 h. Viability of SW1990 (F) and PANC-1 (G) cells with *OLA1* overexpression after GEM treatment for 72 h. Viability of PANC-1 (H) and BxPC-3 (I) cells with *OLA1* knockdown after PTX treatment for 72 h.

(J) Viability of SW1990 cells with *OLA1* overexpression after GEM treatment for 72 h.

(K) Expression of GEM-resistance-related genes in PANC-1 cells with *OLA1* knockdown.

(L) Venn diagram depicting the ABC transporter family in the transcriptional sequencing of acquired drug-resistant cells BxGR and OLA1 knockdown cells.

(M) Western blot analysis of OLA1 protein in SW1990 doxycycline-inducible *OLA1*-overexpression (OLA1^{iOE}) cells.

(N) Flow chart of the subcutaneous transplantation of *OLA1*-overexpressing tumor cells. Body weight (O), tumor size (P), tumor volume (Q), and tumor weight (R) in mice with subcutaneous tumor transplantation.

(S) Ratio of OLA1^{iOE} and vector group between GEM and saline treatment groups, respectively.

(T) Immunohistochemistry analysis of OLA1 and Ki67, and HE is staining in subcutaneous transplantation experiments, Scale bar is 100 μm (left) and 50 μm (right).

n.s., not significant; *$p < 0.05$; **$p < 0.01$; ***$p < 0.001$.

notable overexpression in BxGR cells (Figure 3A). Subsequent Ingenuity Pathway Analysis (IPA) unveiled a gene network wherein OLA1 directly targeted SOX2 (Figure S4A). Corroborating this finding, analysis using the GEPIA2 database demonstrated a high correlation between OLA1 and SOX2 in pancreatic ductal adenocarcinoma (PDAC) (Spearman's r = 0.61; Figure S4B).

Furthermore, mRNA levels of SOX2 and other stemness-related genes (POU5F1, NANOG, and PON1) were observed to be downregulated in OLA1-silenced cells (Figure 3B). These findings were further validated through western blot analysis, which revealed the elevated expression of SOX2 and Oct4 in OLA1-overexpressing cells, while the converse effect was observed in OLA1-knockdown cells (Figure 3C).

To investigate the role of OLA1 in the formation of CSCs, we examined tumor-sphere formation after knockdown of *OLA1*. Tumor microspheres were smaller and fewer in PANC-1 (Figures 3D and 3E) and BxPC-3 cells with *OLA1* knockdown (Figure S4C), while the reverse result was observed in SW1990 *OLA1*-overexpressing cells (Figures 3D and 3E). Similar results were achieved by scanning electron microscopy (SEM) analysis in the OLA1 knocked-down PANC-1 cells (Figure 3D). We isolated tumor spheres from PANC-1, BxPC-3, and SW1990 cells using a serum-free floating-culture system, and showed that *OLA1* mRNA levels were higher than in the parent cells (Figure 3F). To further confirm the effect on the formation of OLA1-induced stemness, stem cell markers (CD44 and CD133) were detected by flow cytometry. Silenced OLA1 attenuated the CD44^{+} and CD133+ fraction in PANC-1, SW1990 and BxPC-3 cells (Figure 3G and 3H). Similarly, the knockdown of *OLA1* also reduced the expression of CD44 and CD133 in SW1990 and BxPC-3 cells (Figures 3I–3L).

Obg-like ATPase 1 binds directly to Sonic Hedgehog and Hedgehog-interacting protein complex

To mechanistically understand the role of OLA1 in Gem resistance, SW1990 cell lines with doxycycline-inducible C-terminal FLAG-tagged OLA1 (Flag-OLA1) were constructed and confirmed by Coomassie blue stain (Figure S5A). A band showing interaction with OLA1 was isolated, analyzed by mass spectrometry, and identified as HHIP (Figure S5B). HHIP is a critical inhibitor of the Hedgehog pathway, its function in chemoresistance is unclear, and an association with OLA1 has not been reported.

To further explore the interaction between OLA1 and HHIP, we detected the mRNA expression level of the protein obtained by mass spectrometry in PANC-1 cells with OLA1 knocked down. Knocked-down of OLA1 enhanced the expression of *HHIP*, *KMT5B*, and *LCN1* remarkably (Figure 4A).

The interaction between OLA1 and HHIP was further confirmed by transient transfection followed by IP and immunoblotting. HEK293T cells were co-transfected with Flag-tagged OLA1, cell lysates were immunoprecipitated using an anti-Flag antibody, and the precipitates were probed with anti-Flag antibodies. HHIP co-precipitated with exogenous Flag-OLA1 (Figure 4B). Co-IP experiments using OLA1 or HHIP antibodies co-precipitated both proteins successfully (Figures 4C and 4D). These results indicated that HHIP interacted with OLA1. To determine whether HHIP bound directly to OLA1, we purified prokaryote-expressed His-tagged OLA1 and OLA1-ΔΔTGS protein and incubated them with cell lysis solution for co-precipitation analysis (Figures 4E and S5C). The results showed that HHIP bound indirectly to OLA1 (Figure S5D). OLA1 and HHIP co-localized in the nucleus, as shown by immunofluorescence co-localization analysis (Figure 4E). HHIP interacts with Hh pathway signal molecule ligands, such as SHH, IHH, and DHH, and we thus speculated that OLA1 might interact with these ligands. It was found that the knockdown of OLA1 resulted in a significant decrease in the endogenous level of SHH but not in IHH and DHH, which was also confirmed by RNA sequencing through the DO enrichment analysis of GASTROINTESTINAL_STROMAL_TUMOR (Figure 4F). Correlationship of OLA1 and SHH in PDAC was also confirmed by Spearman analysis using the GEPIA2 database (r = 0.74) (Figure 4G). We conducted an *in vitro* His-tag pulldown experiment utilizing prokaryotic overexpression OLAI vectors, which revealed that OLA1 indeed bound to SHH (Figures 4H and 4I). Additionally, further *in vitro* interaction tests were conducted using truncated SHH protein and OLA1-flag protein, demonstrating the direct targeting of SHH by OLA1 within the SHH (aa198-462) region (Figure 4J).

Obg-like ATPase 1 reduced gemcitabine sensitivity in pancreatic ductal adenocarcinoma cells by co-activation with Sonic Hedgehog/Hedgehog-interacting protein cascades

To further understand the regulatory role of OLA1-SHH axis in the Gem resistance of pancreatic cancer cells, a series of *in vitro* experiments were performed. We assessed the potential influence of OLA1 on Hh pathways and found that *OLA1* knockdown significantly decreased

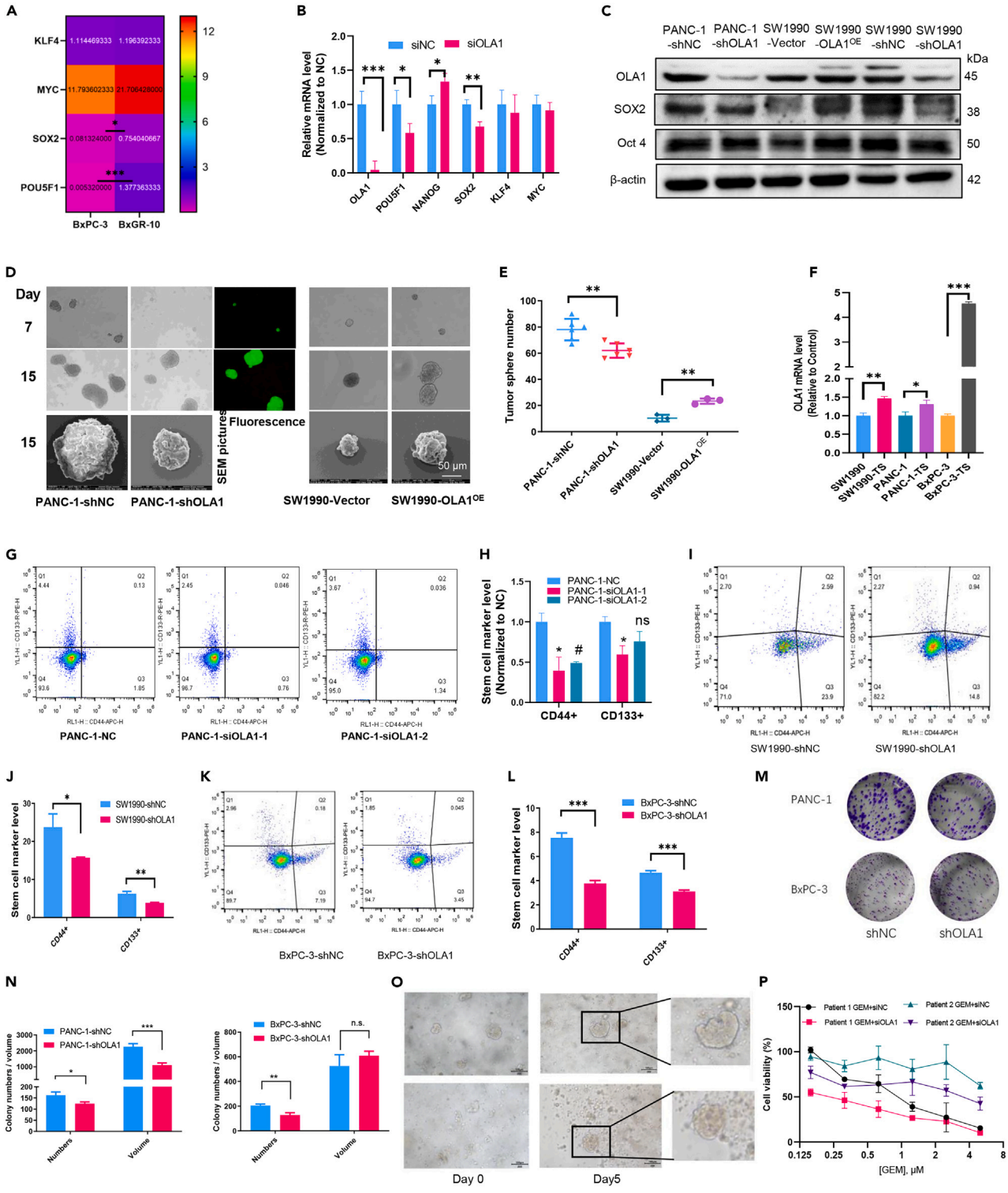

Figure 3. OLA1 induced CSC characteristics

(A) Transcriptomic profiling of stemness gene expression in acquired drug-resistant cells, focusing on OLA1.

(B) mRNA expression levels of cell stemness-related genes in *OLA1*-silenced cells.

(C) Expression levels of cell stemness-related proteins in *OLA1*-knockdown and -overexpressing cells.

Figure 3. *Continued*

(D) Microscopic and electron microscopic images were captured to visualize tumor microsphere formation in OLA1 knockdown and overexpressed cells. Scale bars of 50 μm were included for reference.

(E)Tumor microsphere numbers in *OLA1*-knockdown and -overexpressing cells.

(F) Expression of *OLA1* gene in tumor microspheres.

(G and H) Proportions of $CD44^+$ and CD133+ cells in *OLA1*-silenced cells. Proportions of $CD44^+$ and CD133+ cells in SW1990 (I and J) and BxPC-3 (K and L) *OLA1*-knockdown cells.

(M) Colony-forming ability was assessed in OLA1-knockdown cells. Additionally, tumor microsphere formation was observed in OLA1-knockdown BxPC-3 cells (N).

(O) A diagram depicting pancreatic cancer organoid culture was also included. Scale bars of 100 μm were included for reference.

(P) The impact of knocking down OLA1 on chemotherapy sensitivity in pancreatic cancer was evaluated (P). $^*p < 0.05$; $^{**}p < 0.01$; $^{***}p < 0.001$.

mRNA expression levels of *GLI1*, *GLI3,* and *SHH* in PANC-1 cells (Figure 5A). In line with the mRNA results, the protein expression level of Gli1, as an active marker of Hh, was also reduced by *OLA1* depletion (Figure 5B). Notably, HHIP was highly expressed after *OLA1* knockdown in cell lysates from PANC-1 and BxPC-3 cells, but was down-regulated in the nucleus (Figure 5B). In contrast, *OLA1* overexpression increased the expression levels of Gli1 and SHH and down-regulated HHIP (Figure 5C). In order to further verify the effect of OLA1 on HHIP expression *in vivo*, we conducted protein expression detection in tumor tissues of OLA1-induced over-expression subcutaneous tumor model. HHIP expression was significantly down-regulated in tumor tissues that induced the overexpression of OLA1 (Figure 5D). To further investigate whether OLA1-induced GEM resistance through the hedgehog pathway, the Hedgehog inhibitors Vismodegib (GDC-0449) were utilized, which showed that the remarkable suppression of OLA1 resulted in reduced cell viability (Figure 5E). To further verify the regulatory effects of Vismodegib on OLA1-mediated GEM chemoresistance, a subcutaneous tumor transplantation was performed in NOD-SCID mice using PANC-1 cells with or without the depletion of OLA1. OLA1 suppression by GDC-0449 showed a reduction of the tumor-forming ability, an enhancement of the Gem sensitivity, and a shorteness of the survival time, significantly, in mice treated with GEM (Figures 5F–5H). Immunohistochemistry (IHC) analyses showed that the endogenous level of Ki67, SHH, GLI1, and HHIP was enhanced tremendously in pancreatic cancer cell lines with OLA1 overexpressed (Figures 5I and 5J). Together, the results suggest that OLA1-mediated GEM resistance of pancreatic cancer may be mainly undertaken by the regulation of the OLA1-SHH-HHIP axes in the Hh signaling.

DISCUSSION

CSCs are characterized by a stem cell-like state with retained self-renewal properties, have proven to play key factors in chemoresistance and recurrence of the disease following chemotherapy.[36–38] The residual population of tumor recurrence and chemotherapy-resistant cells was enriched in CSCs.[39] Tumor microenvironment (TME) heterogeneity resulted from CSCs having, to some extent, different ability to be differentiated. TME is dynamic, with spatial and temporal changes in composition in response to environmental pressures and anticancer therapies.[40]

OLA1 has been reported to be related to tumor progression, cellular stress response, drug sensitivity, and centrosome regulation in various cancers.[15,18,20,32] However, the regulatory role of OLA1 in cellular metabolism, CSCs, and especially pancreatic cancer remains unclear. Indeed, CSCs exhibited enhanced spheroid formation and augmented tumor-initiating potential in preclinical models. $CD44^+$, CD133+ are hallmarks of pancreatic cancer, and knockdown of *OLA1* reduced the expression of these markers on the surface of pancreatic cancer cells, and reduced the cells' abilities to form clones and tumor microspheres. CSCs are often regulated by transcription factors, including Oct4, SOX2, Nanog, and kinesin family members. SOX2 is a vital stem cell factor crucial for regulating tumor cell stemness. Transcriptomic sequencing and western blot results accordingly showed that SOX2 was significantly down-regulated in *OLA1*-knockdown cells. IPA gene pathway analysis and transcriptomics sequencing showed that *OLA1* was related to SOX2 and POU5F1 expression changes. Immunoblotting experiments showed that the knockdown of *OLA1* led to a corresponding decrease in the expression of SOX2 and Oct4, while these were increased in cells overexpressing *OLA1*. *SOX2* has also been shown to participate in the Hh pathway by regulating tumor cell stemness to mediate the resistance of pancreatic cancer cells to GEM.[41] These results indicated that OLA1 was closely related to tumor cell stemness.

Analysis of clinical data showed that *OLA1* expression was significantly associated with survival time and chemotherapy resistance in patients with pancreatic cancer, and cell viability results indicated that *OLA1* was associated with GEM and PTX resistance *in vitro*. *OLA1* expression was significantly increased in cells induced by GEM, and cell sensitivity to GEM and PTX was increased dramatically by knockdown of *OLA1*, while the overexpression of *OLA1* had the opposite effect. *RMM1* and *CDA* are essential marker genes for GEM resistance; however, *OLA1* knockdown did not affect the expression levels of these two genes in the current study, suggesting that the *OLA1*-mediated resistance mechanism may differ from traditional GEM resistance affecting the synthesis of cytosine nucleoside. Regarding the mechanism of OLA1-mediated PTX resistance, we previously showed that OLA1 targeted tubulin-induced microtubule depolymerization to alleviate the over-polymerization of microtubules induced by PTX drugs and promote drug resistance in breast cancer cells.[32] In our study, subcutaneous tumor transplantation experiments in Balb/c-nude mice demonstrated that *OLA1* overexpression promoted tumor cell proliferation and GEM tolerance *in vivo*.

Hh is a canonical developmental pathway involved in organogenesis, stem cell maintenance, and tissue repair or regeneration.[42–44] Aberrant Hh signaling is associated with the development and progression of various types of cancer and has been implicated in multiple aspects of tumorigenesis, including the maintenance of CSCs.[45] Hh signaling is activated by binding of its ligands, such as Desert Hedgehog (DHH), Indian Hedgehog (IHH), and sonic Hedgehog (SHH), to their cognate receptors, Patched (Ptch1 and, to a lesser extent, Ptch2).[44] A series of

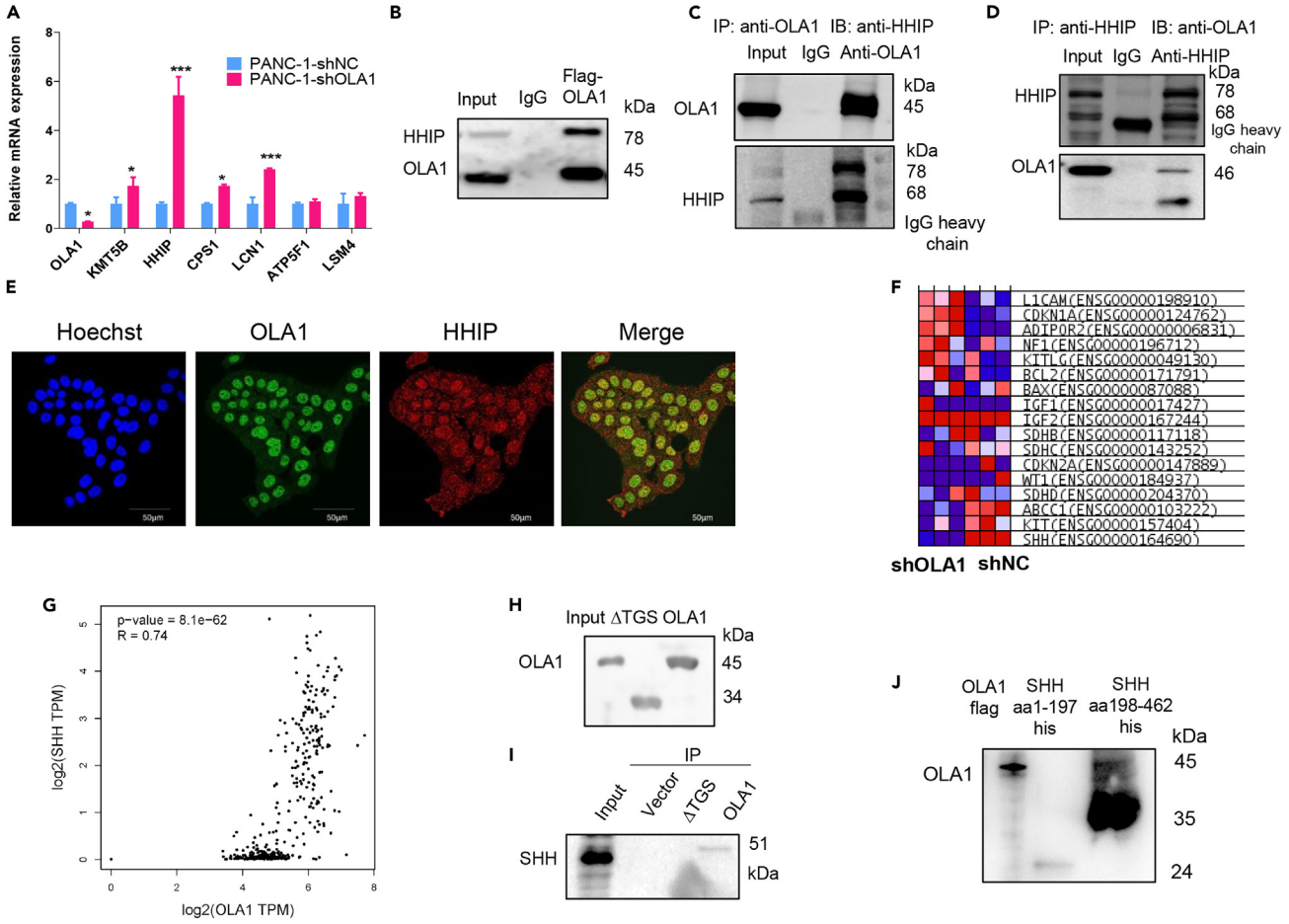

Figure 4. OLA1 binds directly to SHH and HHIP complex

(A) mRNA expression of co-IP-related genes in *OLA1*-knockdown cells.

(B) Co-IP of exogenous OLA1 and HHIP proteins.

(C) Co-IP with OLA1 and (D) HHIP antibodies.

(E) Fluorescence co-localization of OLA1 and HHIP was investigated.

(F) Transcriptome sequencing data for OLA1 was subjected to enrichment analysis focusing on stemness genes.

(G) Spearman's correlation analysis was conducted to examine the relationship between OLA1 and SHH.

(H) Western blot analysis of OLA1 and OLA1-TGS proteins expressed in *Escherichia coli*.

(G) (I) Co-immunoprecipitation (Co-IP) experiments were conducted to examine the interaction between OLA1 and ΔTGS truncated proteins with SHH protein in prokaryotic cells (J) The interaction between OLA1-flag protein and SHH truncate protein was investigated $*p < 0.05$; $***p < 0.001$.

processes facilitate the release of full-length transcriptionally active Gli proteins (GliA) from the suppressor of fused, and GliA then translocates into the nucleus to activate the Hh-targeted genes, such as *PTCH1*, *GLI1*, and *HHIP*, thereby forming feedback loops that reduce or enhance the Hh response.[46]

Mass spectrometric analysis of immunoprecipitated proteins revealed that OLA1 interacted with HHIP. HHIP is a negative regulator of the Hh pathway related to embryonic development and tumor cell stemness. Co-IP, His-pulldown, and colocalization experiments showed that OLA1 and HHIP interacted indirectly and co-localized in the nucleus. Hh is involved in the process of the embryonic development and mediation of drug resistance in tumor cells. SHH is a crucial starting ligand of the Hh pathway and is essential for pathway activation. As the interacting protein of SHH, HHIP is a critical inhibitor of the Hh pathway. OLA1 forms a ternary complex with SHH and HHIP in the nucleus, which enhances the expression of HHIP in the nucleus and inhibits the negative feedback regulation of the Hh pathway. These findings suggest that targeting *OLA1* may be a potential therapeutic approach for sensitizing pancreatic cancer tumors to GEM *in vivo*. Overall, these findings indicate an essential role of OLA1 in CSC-induced drug resistance in PDAC.

Sophisticated changes in the tumor microenvironment shape the heterogeneity of tumor stem cells. In the perception of external stimuli and stress conditions, OLA1 has been reported to have outstanding advantages, not only can sense nutrient deficiency, temperature change, and DNA damage repair. We now report that OLA1 can apperceive GEM stimulation, regulate Hedgehog negative feedback and tumor cell

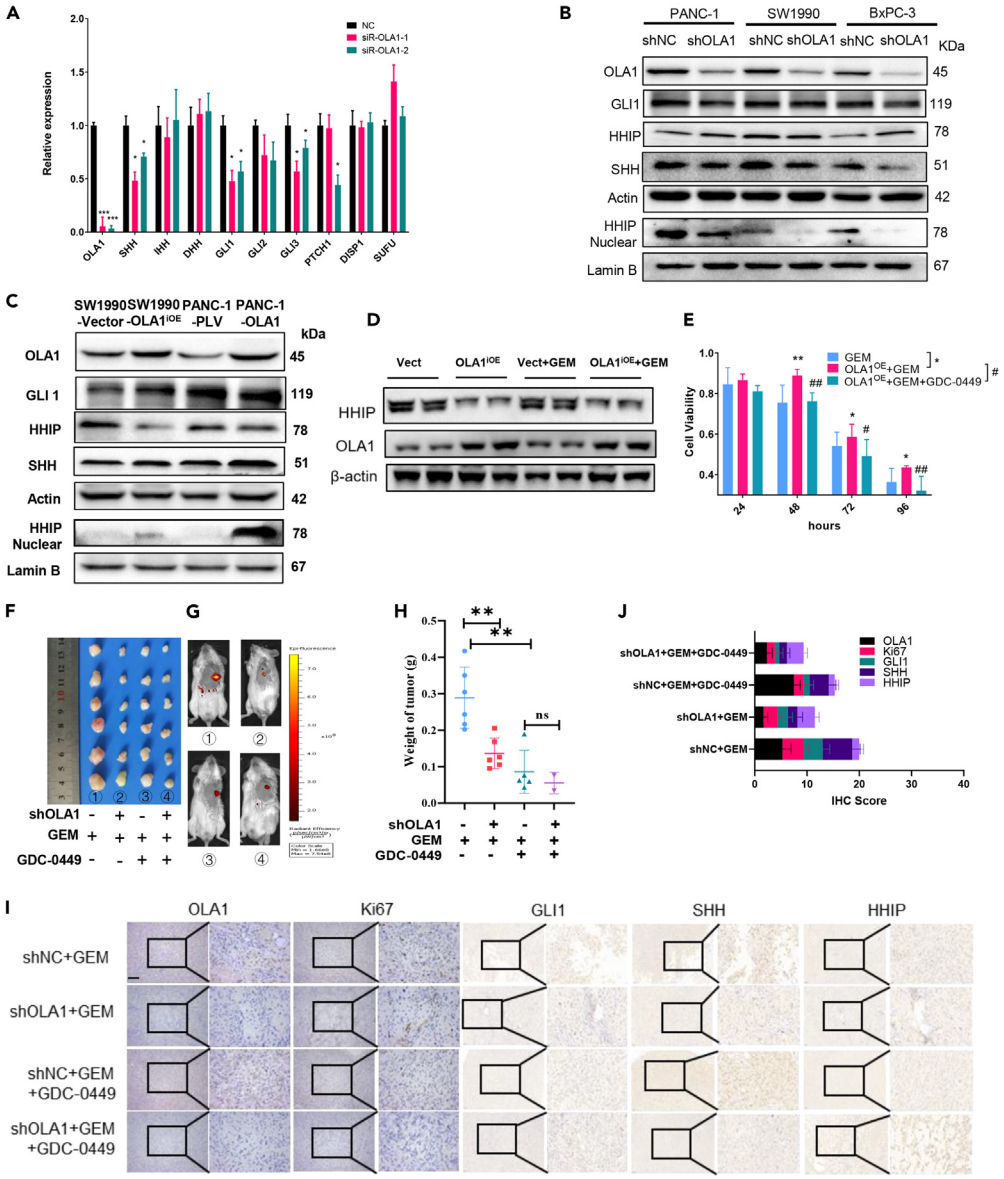

Figure 5. OLA1 reduced the GEM sensitivity of PDAC by the SHH/HHIP axis to activate Hh pathway

(A) Effects of silencing *OLA1* on Hh pathway genes.

(B) Effects of *OLA1* knockdown and (C) overexpression on Hh pathway proteins.

(D) Expression of OLA1 and HHIP in OLA1-induced subcutaneous tumor model.

(E) Effects of GEM and GDC-0449 on the viability of *OLA1*-overexpressing cells. Subsequent analyses included tumor photos (F) and measurements of tumor weight (G) in mice with subcutaneous tumor xenografts. Additionally, animal tumor imaging was performed to assess tumor size and weight (H).

(I and J) Immunohistochemical (IHC) staining was conducted to evaluate the expression of OLA1, Ki67, SHH, Gli1, and HHIP in tumor tissues. Scale bars of 100 μm (left) and 50 μm (right) were included for reference. n.s., not significant; *$p < 0.05$; **$p < 0.01$; ***$p < 0.001$.

stemness through OLA1-SHH nuclear translocation, and promote the generation of tumor drug resistance in pancreatic cancer. OLA1 phosphorylation may be impaired endothelial mitochondrial distress signal was reported,[24] phosphorylation sites coupling ATPase/GTPase functional change, the tumor microenvironment remodeling may also play an important role.

Limitations of the study

The limitation of this article is that we do not have an in-depth analysis of the mechanism by which OLA1 is translocated, and we suspect that it is likely through the phosphorylation of OLA1 at Ser232/Tyr236. In addition, our future research will focus on how OLA1 causes changes in corresponding genotypes through the metabolic reprogramming of tumor microenvironment.

STAR★METHODS

Detailed methods are provided in the online version of this paper and include the following:

SUPPLEMENTAL INFORMATION

Supplemental information can be found online at https://doi.org/10.1016/j.isci.2024.110027.

ACKNOWLEDGMENTS

This study was supported by the Fundamental Research Funds for the Central Universities of China (3332022004 to J. Liu), the National Natural Science Foundation of China (81770846 to G. Xiao), Hirshberg Foundation for Pancreatic Cancer Research of United States (GX20191005878 to G. Xiao), CAMS Innovation Fund for Medical Sciences (CIFMS) of China (2021-I2M-1-002 & 2022-I2M-C&T-B-030 to J. Guo). We also thank Susan Furness, PhD, from Liwen Bianji (Edanz) (www.liwenbianji.cn) for editing the English text of a draft of this article.

AUTHOR CONTRIBUTIONS

J. Liu: data curation, formal analysis, investigation, visualization, methodology, validation, funding acquisition, and writing-original draft. J. Lu, J. Huang: data curation, validation, investigation, and visualization. R. Ouyang: software, visualization, methodology, and writing review. C. Wu: data curation, formal analysis, validation, and investigation. W. Xu, J. Zhang, K. Xiao: software, investigation. D. Shang: data curation, investigation, and visualization. V. Go: conceptualization and formal analysis. J. Guo: resources, data curation, methodology, supervision, funding acquisition, project administration, and writing review and editing. G. Xiao: conceptualization, resources, data curation, formal analysis, supervision, funding acquisition, validation, investigation, visualization, methodology, project administration, and writing review and editing.

DECLARATION OF INTERESTS

The authors declare no competing interests.

Received: November 22, 2023
Revised: April 1, 2024
Accepted: May 16, 2024
Published: May 21, 2024

REFERENCES

1. Encarnación-Rosado, J., and Kimmelman, A.C. (2021). Harnessing metabolic dependencies in pancreatic cancers. Nat. Rev. Gastroenterol. Hepatol. *18*, 482–492. https://doi.org/10.1038/s41575-021-00431-7.
2. Mizrahi, J.D., Surana, R., Valle, J.W., and Shroff, R.T. (2020). Pancreatic cancer. Lancet (London, England) *395*, 2008–2020. https://doi.org/10.1016/s0140-6736(20)30974-0.
3. Siegel, R.L., Miller, K.D., Wagle, N.S., and Jemal, A. (2023). Cancer statistics, 2023. CA A Cancer J. Clin. *73*, 17–48. https://doi.org/10.3322/caac.21763.
4. Wu, W., Miao, Y., Yang, Y., Lou, W., and Zhao, Y. (2022). Real-world study of surgical treatment of pancreatic cancer in China: annual report of China Pancreas Data Center (2016-2020). J. Pancreatol. *5*, 1–9. https://doi.org/10.1097/JP9.0000000000000086.
5. Shi, Y., Gao, W., Lytle, N.K., Huang, P., Yuan, X., Dann, A.M., Ridinger-Saison, M., DelGiorno, K.E., Antal, C.E., Liang, G., et al. (2019). Targeting LIF-mediated paracrine interaction for pancreatic cancer therapy and monitoring. Nature *569*, 131–135. https://doi.org/10.1038/s41586-019-1130-6.
6. Phi, L.T.H., Sari, I.N., Yang, Y.G., Lee, S.H., Jun, N., Kim, K.S., Lee, Y.K., and Kwon, H.Y. (2018). Cancer Stem Cells (CSCs) in Drug Resistance and their Therapeutic Implications in Cancer Treatment. Stem Cell. Int. *2018*, 5416923. https://doi.org/10.1155/2018/5416923.
7. Pattabiraman, D.R., and Weinberg, R.A. (2014). Tackling the cancer stem cells - what challenges do they pose? Nat. Rev. Drug Discov. *13*, 497–512. https://doi.org/10.1038/nrd4253.
8. Mueller, M.T., Hermann, P.C., Witthauer, J., Rubio-Viqueira, B., Leicht, S.F., Huber, S., Ellwart, J.W., Mustafa, M., Bartenstein, P., D'Haese, J.G., et al. (2009). Combined Targeted Treatment to Eliminate Tumorigenic Cancer Stem Cells in Human Pancreatic Cancer. Gastroenterology *137*, 1102–1113. https://doi.org/10.1053/j.gastro.2009.05.053.
9. Hermann, P.C., Huber, S.L., Herrler, T., Aicher, A., Ellwart, J.W., Guba, M., Bruns, C.J., and Heeschen, C. (2007). Distinct populations of cancer stem cells determine tumor growth and metastatic activity in human pancreatic cancer. Cell Stem Cell *1*, 313–323. https://doi.org/10.1016/j.stem.2007.06.002.
10. Ling, S., Shan, Q., Zhan, Q., Ye, Q., Liu, P., Xu, S., He, X., Ma, J., Xiang, J., Jiang, G., et al. (2020). USP22 promotes hypoxia-induced hepatocellular carcinoma stemness by a HIF1α/USP22 positive feedback loop upon TP53 inactivation. Gut *69*, 1322–1334. https://doi.org/10.1136/gutjnl-2019-319616.
11. Leipe, D.D., Wolf, Y.I., Koonin, E.V., and Aravind, L. (2002). Classification and evolution of P-loop GTPases and related ATPases. J. Mol. Biol. *317*, 41–72. https://doi.org/10.1006/jmbi.2001.5378.
12. Verstraeten, N., Fauvart, M., Versées, W., and Michiels, J. (2011). The Universally Conserved Prokaryotic GTPases. Microbiol. Mol. Biol. Rev. *75*, 507–542. https://doi.org/10.1128/MMBR.00009-11.
13. Gradia, D.F., Rau, K., Umaki, A.C.S., de Souza, F.S.P., Probst, C.M., Correa, A., Holetz, F.B., Avila, A.R., Krieger, M.A., Goldenberg, S., and Fragoso, S.P. (2009). Characterization of a novel Obg-like ATPase in the protozoan Trypanosoma cruzi. Int. J. Parasitol. *39*, 49–58. https://doi.org/10.1016/j.ijpara.2008.05.019.
14. Koller-Eichhorn, R., Marquardt, T., Gail, R., Wittinghofer, A., Kostrewa, D., Kutay, U., and Kambach, C. (2007). Human OLA1 defines an ATPase subfamily in the Obg family of GTP-binding proteins. J. Biol. Chem. *282*, 19928–19937. https://doi.org/10.1074/jbc.M700541200.
15. Ding, Z., Liu, Y., Rubio, V., He, J., Minze, L.J., and Shi, Z.Z. (2016). OLA1, a Translational Regulator of p21, Maintains Optimal Cell Proliferation Necessary for Developmental Progression. Mol. Cell Biol. *36*, 2568–2582. https://doi.org/10.1128/mcb.00137-16.
16. Balasingam, N., Brandon, H.E., Ross, J.A., Wieden, H.J., and Thakor, N. (2020). Cellular roles of the human Obg-like ATPase 1 (hOLA1) and its YchF homologs. Biochem. Cell Biol. *98*, 1–11. https://doi.org/10.1139/bcb-2018-0353.
17. Landwehr, V., Milanov, M., Angebauer, L., Hong, J., Jüngert, G., Hiersemenzel, A., Siebler, A., Schmit, F., Öztürk, Y., Dannenmaier, S., et al. (2021). The Universally Conserved ATPase YchF Regulates Translation of Leaderless mRNA in Response to Stress Conditions. Front. Mol. Biosci. *8*, 643696. https://doi.org/10.3389/fmolb.2021.643696.
18. Liu, Y., Kong, X.X., He, J.J., Xu, Y.B., Zhang, J.K., Zou, L.Y., Ding, K.F., and Xu, D. (2022). OLA1 promotes colorectal cancer tumorigenesis by activation of HIF1α/CA9 axis. BMC Cancer *22*, 424. https://doi.org/10.1186/s12885-022-09508-1.
19. Sun, H., Luo, X., Montalbano, J., Jin, W., Shi, J., Sheikh, M.S., and Huang, Y. (2010). DOC45, a novel DNA damage-regulated nucleocytoplasmic ATPase that is overexpressed in multiple human malignancies. Mol. Cancer Res. *8*, 57–66. https://doi.org/10.1158/1541-7786.MCR-09-0278.
20. Matsuzawa, A., Kanno, S.I., Nakayama, M., Mochiduki, H., Wei, L., Shimaoka, T., Furukawa, Y., Kato, K., Shibata, S., Yasui, A., et al. (2014). The BRCA1/BARD1-interacting protein OLA1 functions in centrosome regulation. Mol. Cell *53*, 101–114. https://doi.org/10.1016/j.molcel.2013.10.028.
21. Yoshino, Y., Qi, H., Kanazawa, R., Sugamata, M., Suzuki, K., Kobayashi, A., Shindo, K., Matsuzawa, A., Shibata, S., Endo, S., et al. (2019). RACK1 regulates centriole duplication by controlling localization of BRCA1 to the centrosome in mammary tissue-derived cells. Oncogene *38*, 3077–3092. https://doi.org/10.1038/s41388-018-0647-8.
22. Fang, Z., Li, X., Yoshino, Y., Suzuki, M., Qi, H., Murooka, H., Katakai, R., Shirota, M., Mai Pham, T.A., Matsuzawa, A., et al. (2023). Aurora A polyubiquitinates the BRCA1-interacting protein OLA1 to promote centrosome maturation. Cell Rep. *42*, 112850. https://doi.org/10.1016/j.celrep.2023.112850.
23. Lu, S., Han, L., Hu, X., Sun, T., Xu, D., Li, Y., Chen, Q., Yao, W., He, M., Wang, Z., et al. (2021). N6-methyladenosine reader IMP2 stabilizes the ZFAS1/OLA1 axis and activates the Warburg effect: implication in colorectal cancer. J. Hematol. Oncol. *14*, 188. https://doi.org/10.1186/s13045-021-01204-0.
24. Sidlowski, P., Czerwinski, A., Liu, Y., Liu, P., Teng, R.J., Kumar, S., Wells, C., Pritchard, K., Jr., Konduri, G.G., and Afolayan, A.J. (2023). OLA1 Phosphorylation Governs the Mitochondrial Bioenergetic Function of Pulmonary Vascular Cells. Am. J. Respir. Cell Mol. Biol. *68*, 395–405. https://doi.org/10.1165/rcmb.2022-0186OC.
25. Huang, S., Zhang, C., Sun, C., Hou, Y., Zhang, Y., Tam, N.L., Wang, Z., Yu, J., Huang, B., Zhuang, H., et al. (2020). Obg-like ATPase 1 (OLA1) overexpression predicts poor prognosis and promotes tumor progression by regulating P21/CDK2 in hepatocellular carcinoma. Aging *12*, 3025–3041. https://doi.org/10.18632/aging.102797.
26. Dong, Y., Yin, A., Xu, C., Jiang, H., Wang, Q., Wu, W., and Guo, S. (2021). OLA1 is a potential prognostic molecular biomarker for endometrial cancer and promotes tumor progression. Oncol. Lett. *22*, 576. https://doi.org/10.3892/ol.2021.12837.
27. Aoki, I., Jurado, P., Nawa, K., Kondo, R., Yamashiro, R., Matsuyama, H.J., Ferrer, I., Nakano, S., and Mori, I. (2022). OLA-1, an Obg-like ATPase, integrates hunger with temperature information in sensory neurons in C. elegans. PLoS Genet. *18*, e1010219. https://doi.org/10.1371/journal.pgen.1010219.
28. Dannenmaier, S., Desroches Altamirano, C., Schüler, L., Zhang, Y., Hummel, J., Milanov, M., Oeljeklaus, S., Koch, H.G., Rospert, S., Alberti, S., and Warscheid, B. (2021). Quantitative proteomics identifies the universally conserved ATPase Ola1p as a positive regulator of heat shock response in Saccharomyces cerevisiae. J. Biol. Chem. *297*, 101050. https://doi.org/10.1016/j.jbc.2021.101050.
29. Lu, J., Jia, J., Zhang, J., and Liu, X. (2021). HIV p17 enhances T cell proliferation by suppressing autophagy through the p17-OLA1-GSK3β axis under nutrient starvation. J. Med. Virol. *93*, 3607–3620. https://doi.org/10.1002/jmv.26423.
30. Zhang, J., Rubio, V., Lieberman, M.W., and Shi, Z.Z. (2009). OLA1, an Obg-like ATPase, suppresses antioxidant response via nontranscriptional mechanisms. Proc. Natl. Acad. Sci. USA *106*, 15356–15361. https://doi.org/10.1073/pnas.0907213106.
31. Landwehr, V., Milanov, M., Hong, J., and Koch, H.G. (2021). The Role of the Universally Conserved ATPase YchF/Ola1 in Translation Regulation during Cellular Stress. Microorganisms *10*, 14. https://doi.org/10.3390/microorganisms10010014.
32. Liu, J., Miao, X., Xiao, B., Huang, J., Tao, X., Zhang, J., Zhao, H., Pan, Y., Wang, H., Gao, G., and Xiao, G.G. (2020). Obg-Like ATPase 1 Enhances Chemoresistance of Breast Cancer via Activation of TGF-β/Smad Axis Cascades. Front. Pharmacol. *11*, 666. https://doi.org/10.3389/fphar.2020.00666.
33. Bai, L., Yu, Z., Zhang, J., Yuan, S., Liao, C., Jeyabal, P.V.S., Rubio, V., Chen, H., Li, Y., and Shi, Z.Z. (2016). OLA1 contributes to epithelial-mesenchymal transition in lung cancer by modulating the GSK3β/snail/E-cadherin signaling. Oncotarget *7*, 10402–10413.
34. Zhang, J.W., Rubio, V., Zheng, S., and Shi, Z.Z. (2009). Knockdown of OLA1, a regulator of oxidative stress response, inhibits motility and invasion of breast cancer cells. J. Zhejiang Univ. - Sci. B *10*, 796–804. https://doi.org/10.1631/jzus.B0910009.
35. Fischer, K.R., Durrans, A., Lee, S., Sheng, J., Li, F., Wong, S.T.C., Choi, H., El Rayes, T., Ryu, S.,

Troeger, J., et al. (2015). Epithelial-to-mesenchymal transition is not required for lung metastasis but contributes to chemoresistance. Nature *527*, 472–476. https://doi.org/10.1038/nature15748.

36. Maugeri-Saccà, M., Vigneri, P., and De Maria, R. (2011). Cancer stem cells and chemosensitivity. Clin. Cancer Res. *17*, 4942–4947. https://doi.org/10.1158/1078-0432.Ccr-10-2538.
37. Zhao, J. (2016). Cancer stem cells and chemoresistance: The smartest survives the raid. Pharmacol. Ther. *160*, 145–158. https://doi.org/10.1016/j.pharmthera.2016.02.008.
38. Xu, C., Li, S., Chen, J., Wang, H., Li, Z., Deng, Q., Li, J., Wang, X., Xiong, Y., Zhang, Z., et al. (2023). Doxorubicin and erastin co-loaded hydroxyethyl starch-polycaprolactone nanoparticles for synergistic cancer therapy. J. Contr. Release *356*, 256–271. https://doi.org/10.1016/j.jconrel.2023.03.001.
39. Batlle, E., and Clevers, H. (2017). Cancer stem cells revisited. Nat. Med. *23*, 1124–1134. https://doi.org/10.1038/nm.4409.
40. Bocci, F., Gearhart-Serna, L., Boareto, M., Ribeiro, M., Ben-Jacob, E., Devi, G.R., Levine, H., Onuchic, J.N., and Jolly, M.K. (2019). Toward understanding cancer stem cell heterogeneity in the tumor microenvironment. Proc. Natl. Acad. Sci. USA *116*, 148–157. https://doi.org/10.1073/pnas.1815345116.
41. Jia, Y., Gu, D., Wan, J., Yu, B., Zhang, X., Chiorean, E.G., Wang, Y., and Xie, J. (2019). The role of GLI-SOX2 signaling axis for gemcitabine resistance in pancreatic cancer. Oncogene *38*, 1764–1777. https://doi.org/10.1038/s41388-018-0553-0.
42. Justilien, V., and Fields, A.P. (2015). Molecular Pathways: Novel Approaches for Improved Therapeutic Targeting of Hedgehog Signaling in Cancer Stem Cells. Clin. Cancer Res. *21*, 505–513. https://doi.org/10.1158/1078-0432.Ccr-14-0507.
43. Su, P.H., Huang, R.L., Lai, H.C., Chen, L.Y., Weng, Y.C., Wang, C.C., and Wu, C.C. (2021). NKX6-1 mediates cancer stem-like properties and regulates sonic hedgehog signaling in leiomyosarcoma. J. Biomed. Sci. *28*, 32. https://doi.org/10.1186/s12929-021-00726-6.
44. Zhang, Y., and Beachy, P.A. (2023). Cellular and molecular mechanisms of Hedgehog signalling. Nat. Rev. Mol. Cell Biol. *24*, 668–687. https://doi.org/10.1038/s41580-023-00591-1.
45. Cochrane, C.R., Szczepny, A., Watkins, D.N., and Cain, J.E. (2015). Hedgehog Signaling in the Maintenance of Cancer Stem Cells. Cancers *7*, 1554–1585. https://doi.org/10.3390/cancers7030851.
46. Zhu, R., Gires, O., Zhu, L., Liu, J., Li, J., Yang, H., Ju, G., Huang, J., Ge, W., Chen, Y., et al. (2019). TSPAN8 promotes cancer cell stemness via activation of sonic Hedgehog signaling. Nat. Commun. *10*, 2863. https://doi.org/10.1038/s41467-019-10739-3.
47. Zhou, C., Yi, C., Yi, Y., Qin, W., Yan, Y., Dong, X., Zhang, X., Huang, Y., Zhang, R., Wei, J., et al. (2020). LncRNA PVT1 promotes gemcitabine resistance of pancreatic cancer via activating Wnt/β-catenin and autophagy pathway through modulating the miR-619-5p/Pygo2 and miR-619-5p/ATG14 axes. Mol. Cancer *19*, 118. https://doi.org/10.1186/s12943-020-01237-y.

STAR★METHODS

KEY RESOURCES TABLE

REAGENT or RESOURCE	SOURCE	IDENTIFIER
Antibodies		
GTPBP9	Invitrogen	#PA5-31227; RRID: AB_2548701
Actin	Invitrogen	#PA5-78715; RRID: AB_2745831
GAPDH	Cell Signaling Technology	#5174; RRID: AB_10622025
Hedgehog antibody kit	Cell Signaling Technology	#26118; RRID: NA
Human SHH (aa1-197)	Sino Biological	#10372-H08H1; RRID: NA
Human SHH (aa198-462)	Sino Biological	#10372-H08H; RRID: NA
SOX2	ABclonal	#A11501; RRID: AB_2758586
CD44	BD. Biosciences	#559942; RRID: AB_398683
CD133	BD. Biosciences	#566593; RRID: AB_2744281
HHIP	Novus Biologicals	#H00064399-M01; RRID: AB_2295202
Lamin B	ProteinTech Inc	#12987-1-AP; RRID: AB_2136290
Second antibody	Abbkine Inc	#A21010; RRID: AB_2728771, #A25022; RRID: AB_2893334
Chemicals, peptides, and recombinant proteins		
Gemcitabine	Selleck.cn	#S1149
Paclitaxel	Selleck.cn	#S1150
GDC-0449	Selleck.cn	#S1082
MTT	Solarbio Inc	#M8180
silence negative control	Sigma-Aldrich	#SIC001
siOLA1	Sigma-Aldrich	#SASI_Hs01_00244684
Lipofectamine™ 3000	Thermo Scientific	#L3000001
Y-27632	Sigma-Aldrich	#146986-50-7
Stain Buffer	BD. Biosciences	#554656
B-27™ Supplement	ThermoFisher	#A1895601
Matrigel	ThermoFisher	#354234
ECL	Applygen Technologies Inc.	#P1010
RIPA lysis buffer	Applygen Technologies Inc.	#C1053
DMEM	Gibco	N/A
RPMI 1640	Gibco	N/A
Horse serum	Gibco	#16050122
Fetal Bovine Serum	Gibco	#16140071
Penicillin & Streptomycin	Solarbio Inc	#P1400
TRIzol	Invitrogen	#15596026
Critical commercial assays		
BCA Kit	Solarbio Inc	#PC0020
PrimeScriptTM RT Reagent Kit	Takara	#RR037A
PrimeSTAR® Max DNA Polymerase Kit	Takara	#R045A
Experimental models: Cell lines		
PANC-1	ATCC	#CRL-1469
BxPC-3	ATCC	CRL-1687
SW1990	ATCC	CRL-2172

(*Continued on next page*)

Continued

REAGENT or RESOURCE	SOURCE	IDENTIFIER
AsPC-1	ATCC	CRL-1682
MIA PaCa-2	ATCC	CRM-CRL-1420
HPAF-II	ATCC	CRL-1997
CFPAC-1	ATCC	CRL-1918
Capan-2	ATCC	HTB-80
HPDE6-C7	Donated by Prof. Zhengzheng Shi	N/A
Experimental models: Organisms/strains		
BALB/c nude mice	Beijing Vital River Laboratory Animal Technology Co., Ltd.	N/A
Small hairpin RNA (shRNA) lentiviral	GenePharma	N/A
pGLV3/H1/GFP/Puro vector plasmid	GenePharma	N/A
Tet-on system, pLV-TRE-OLA1 (human) -flag-IRES-EYFP-hef1a-rtTA-P2A-Puro	SyngenTech, Beijing, China	N/A
pdEYFP-N1gen plasmid with a C-terminal YFP tag, $OLA1^{OE}$	Donated by Prof. Zhengzheng Shi	N/A
OLA1-Flag plasmid (pIRESneo3-FLAG vector)	Donated by Prof. Zhengzheng Shi	N/A
Oligonucleotides		
Hu-GAPDH-F: CATGAGAAGTATGACAACAGCCT	Tsingke.com	N/A
Hu-GAPDH-R: AGTCCTTCCACGATACCAAAGT	Tsingke.com	N/A
Hu-OLA1-F: TGGACAAGTATGACCCAGGT	Tsingke.com	N/A
Hu-OLA1-R: GCTGCAAACCCAGCCTTAATG	Tsingke.com	N/A
Software and algorithms		
GraphPad Prism 8.0.2.263	GraphPad Software	https://www.graphpad.com/
ImageJ	NIH	RRID: SRC_003070
SPSS 25.0	IBM	http://www.spss.com.cn
Adobe Illustrator	Adobe	https://www.adobe.com/
Others		
NanoDrop	Thermo Fisher Scientific	NanoDrop One Microvolume UV-Vis Spectrophotometers
Real-Time PCR machine	Roche	480II
Microplate reader	Agilent	BioTek Synergy H1 Multimode Reader

RESOURCE AVAILABILITY

Lead contact

Further information and requests for resources and reagents should be directed to and will be fulfilled by the lead contact, Junchao Guo (gjcpumch@163.com).

Materials availability

This study did not generate new unique reagents.

Data and code availability

All data generated or analyzed during this study are included in this published article (and its supplemental information) and can be made available upon reasonable request. Any additional information required to reanalyze the data reported in this paper is available from the lead contact upon request.

This paper does not report original code.

EXPERIMENTAL MODEL AND STUDY PARTICIPANT DETAILS

Patients and tissue samples

PDAC and adjacent normal tissues were obtained from 265 Asian patients who underwent radical surgical resection without neoadjuvant therapy. The diagnosis of PDAC was confirmed pathologically due to the World Health Organization criteria. The patients comprised 154 men and 111 women. The clinicopathological data included patient demographics (age and gender), tumor location, tumor size, CA19-9 level, histological grade, perineural invasion, tumor T stage, lymph node N stage, metastasis stage, chemotherapy responses and cancer-specific survival time. The clinicopathological characteristics of the patients are shown in Table 1.

Ethics statement

All animal studies were done according to the approved protocol of the Animal Experimental Ethical Committee of Dalian Medical University (NO. AEE19085) and Peking Union Medical College Hospital Ethical Committee (NO. XHDW-2022-165). The patients' tissue array for the OLA1 research was approved by the Peking Union Medical College Hospital Ethical Committee and informed consent was obtained from all patients.

In vitro organoid study

We established two pancreatic tumor organoid lines using fresh patient pancreatic tumor samples. Informed consent was acquired from participants, and approval of the experimental protocol was obtained from the medical ethics committee of PUMCH. Tumor tissues were transported directly from the operating room to the laboratory for processing, where they were divided into pieces for organoid culture. New surgical tissues were washed with Hanks' balanced salt solution (HBSS) supplemented with penicillin/streptomycin and 10 μM Y-27632 (a ROCK inhibitor), scissored into 1 mm^3 pieces, and then enzymatically dissociated using a tissue pre-treatment kit (Accurate Int., Guangzhou). The collected cells were washed and re-suspended in advanced Dulbecco's modified Eagle medium (DMEM)/F12 and embedded in growth factor-reduced Matrigel at a ratio of 1:1.5. The dome was incubated at 37°C for 30 min. After solidification, the organoid culture medium was added and replenished every 3–4 days, which contained advanced DMEM/F12, 1× GlutaMax, 1× B27, 10 mM nicotinamide, 1.25 mM N-acetyl cysteine, 20 mM 4-(2-hydroxyethyl)-1-piperazineëthanesulfonic acid (HEPES), 10 nM gastrin, 5 $ng{\cdot}mL^{-1}$ fibroblast growth factor (FGF)-basic, 15 ng·mL-1 FGF-10, 50 ng·mL-1 epidermal growth factor (EGF), 100 $ng{\cdot}mL^{-1}$ Wnt3a, 100 $ng{\cdot}mL^{-1}$ Noggin, 100 $ng{\cdot}mL^{-1}$ R-spondin-1, 500 nM A83-01, 10 μM SB220190, and 10 μM Y-27632. Passages of organoids were performed every 7–14 days at a split ratio of 1:1–1:5. Biobanking of organoids was achieved by cryopreservation in 10% DMSO/FBS solution under liquid nitrogen.

Cell culture

Human PANC-1, BxPC-3, SW1990, AsPC-1, MIA-PaCa-2, HPAF-II, CFPAC-1, Capan-2 pancreatic carcinoma cells and Human normal pancreatic ductal epithelial cells (HPDE6-C7) were from the Institute of Biochemistry and Cell Biology, Chinese Academy of Sciences (IBCB, Shanghai, China), were routinely grown in Dulbecco's modified Eagle's medium (DMEM; Gibco, Rockville, MD, USA) or RPMI 1640 Medium (Gibco, Rockville, MD, USA) containing 10 % fetal bovine serum (P.A.N., Germany) or 10% horse serum (Gibco, Rockville, MD, USA) for MIA-PaCa-2, 100 IU/ml penicillin and 100 μg/ml streptomycin (Solarbio, Beijing, China) in an incubator at 37°C, 5% CO_2. The GEM-resistant sublines (BxGR) were derived from BxPC-3 by continuous exposure to G.E.M. BxGR cells were cultured continuously in a medium containing 10% FBS supplemented with 100 nM GEM All cell lines were checked by STR profiling and mycoplasma was tested every two months.

METHOD DETAILS

Cell viability assay

Cell viability was determined by MTT assay performed as described.[47] In brief, the cells were seeded onto 96-well plates and incubated overnight at 37°C. GEM at different concentrations was added to each well with varying incubation times. After that, 20 μL MTT solution (5 mg/mL) was added to each well. The absorbance was measured at 490nm by the microplate reader. Six replicate wells were included in each analysis and at least three independent experiments were conducted. The cell inhibition rate and IC50 were calculated respectively by SPSS. The same method was used for the measurement of PTX.

Cell proliferation

Cell proliferation ability was also assessed using an MTT assay. The silence group was transfected with either siOLA1 or silence negative control (siNC) for 12 h before use. In the experimental group transfected with interfering RNA, the culture medium containing the transfection reagent and the interfering RNA will be replaced once on the fourth day of the experiment. Cells, on days 1, 2, 3, 4, 5, 6, 7 and 8, respectively, were incubated with MTT solution. Six replicate wells were included in each analysis and at least three independent experiments were conducted.

Development of GEM resistant cell lines

Low-concentration induction method was used to construct drug-resistant cell lines. Briefly, the IC_{50} of paclitaxel on BxPC-3 was detected, and the appropriate initial concentration (20 nM) was selected and added to the culture flask for incubation. After 24 h, the medicated medium

was aspirated, washed with PBS, and added to the regular medium until the cells were over 80% and passaged. Incubate with an equal concentration of the drug depending on cell growth, or add a four-fold drug dose. Cycle back and forth until the resistance meets the experimental needs. The establishment cycle of acquired drug-resistant cells is about six months.

Library preparation for transcriptome sequencing

The library preparation for transcriptome sequencing involved the utilization of conventional Illumina second-generation sequencing technology to sequence OLA1-knockdown cells and acquired resistance cells. Each cell group was comprised of three parallel samples for robust analysis.

Small interfering RNA transfections

Small interfering RNA (siRNA) for OLA1 (SASI_Hs01_00244684) and the control siRNA (MISSON siRNA Universal Negative Control #1 SIC001) were purchased from Sigma-Aldrich. According to the manufacturer's instructions, cells seeded in a 6-well plate were transiently transfected with 100 pM siRNA with the Lipo2000 Transfection Reagent (Thermo Scientific).

Establishment of the stable OLA1 knockdown pancreatic cancer cell lines

Small hairpin RNA (shRNA) lentiviral used for stable silencing of OLA1 (shOLA1) and the control non-targeting plasmid (shNC) were purchased from GenePharma (Shanghai, China) by inserting the following short-hairpin sequences into the pGLV3/H1/GFP/Puro vector: 5′-**TGTTCGCTTCCAGATACTT**-3′ for shOLA1 and 5′-**TTCTCCGAACGTGTCACGT**-3′ for Small hairpin normal control (shNC). The shNC and shOLA1 vectors were transfected into three cancer cells. The knockdown efficiency of the target gene was verified by qRT-PCR and western blot analysis. Small hairpin RNA (shRNA) transfections and protocol followed the recommendations by GenePharma (China).

Development of OLA1 *Tet-On* system

Using the *Tet-on* system, we constructed the tetracycline-induced OLA1 overexpression plasmid ($OLA1^{iOE}$) pLV-TRE-OLA1 (human) -flag-IRES-EYFP-hef1a-rtTA-P2A-Puro (SyngenTech, Beijing, China). The plasmid was successfully constructed after sequence determination and transfection-induced expression verification.

Construction of OLA1 stable overexpression or N230 mutation cell line

OLA1-YFP plasmid (pdEYFP-N1gen plasmid with a C-terminal YFP tag, $OLA1^{OE}$) and OLA1-Flag plasmid (pIRESneo3-FLAG vector), which allow the expression of N-terminal FLAG-tagged wild-type, N230 mutant and ΔTGS (304aa) OLA1proteins were donated by Prof. Zhengzheng Shi. Cells in 6-well plates were transfected with the related plasmid (4 μg DNA/well) or the control plasmid using Lipofectamine 2000 (8 μL/well, Invitrogen).

Formation of cell colony and tumor microsphere

The clone formation experiment used a 6-well plate to cultivate about 200 cells / well in a cell incubator for two weeks. After the clone was formed, the culture solution was discarded, fixed with 4% paraformaldehyde, and stained with Giemsa stain for 20 minutes. After washing the dyeing solution, it is dried and photographed. Tumor microsphere formation experiments were also performed in 6-well plates. Pancreatic cancer cells were cultured to a density of 80% with 10% serum medium, washed three times with PBS, digested with pancreatin for 5-10 minutes, terminated the digestion, centrifuged, washed once with PBS, added serum-free cancer stem medium (CSM, including DMEM/F12, 20 ng/ml EGF, 20 ng/ml FGF, 2% B27, 5 μg/ml insulin) to wait. Tumor cells were photographed under the microscope and counted 7 and 15 days after sphere formation.

Flow cytometry

The apoptosis detection is carried out according to the instructions. Briefly, the cells were trypsinized and centrifuged at 300 g for 5 minutes at 4°C, then washed twice with pre-cooled PBS. Staining cells with binding buffer containing Annexin V-FITC and PI for 10minutes, then detected by a Flow cytometer. The detection of cell stem markers (CD44, CD133) is also carried out following the corresponding antibody instructions (BD Biosciences, San Jose, CA, USA). Briefly, prepare a single cell suspension, wash the cells twice with pre-cooled Stain Buffer, and centrifuge at 300 × g at 4°C. Resuspend the cells with pre-chilled Stain Buffer so that the cell concentration is $2x10^7$ cells / mL. Take 50 μL of cell suspension (10^6 cells) into a 1.5 mL centrifuge tube. Add 5-20 μL of the corresponding antibody to the experimental group, incubate on ice for 30 minutes in the dark, and mix once every 5 minutes. Add 1 mL Stain Buffer to wash twice, 300 × g, centrifuge for 5 mins Resuspend cells with 0.5 mL Stain Buffer. Protect from light and use flow cytometry as soon as possible.

qRT-PCR analysis

Total RNA was extracted from the cells using TRIzol (Cat#15596026, Invitrogen, CA, USA), and the concentration and quality were determined by a microplate reader (DU730, Beckman, CA, USA). The nucleotides were reverse-transcribed into cDNA according to the instructions of the PrimeScriptTM RT Reagent Kit (Cat#RR037A, Takara, Japan). After amplification and dilution, the assay was performed on the LightCycler480

II (Roche, U.S.A.). Gene primer as follows: GAPDH (glyceraldehyde 3-phosphate dehydrogenase): Forward primer: 5-CATGAGAAGTATGA CAACAGCCT Reverse primer: 5-AGTCCTTCCACGATACCAAAGT; OLA1: Forward primer: 5-TGGACAAGTATGACCCAGGT Reverse primer: 5-GCTGCAAACCCAGCCTTAATG.

Western blotting analysis

Protein was extracted from the cells using RIPA buffer, added with PMSF to avoid degrading and stored at -80°C. The BCA protein concentration detection kit was used for quantification, and the loading buffer was added in proportion to boil at 95°C and stored in a refrigerator at -20°C. The SDS-PAGE gel was prepared, and 30 μg of protein sample was added to each lane. The target protein band was cut and transferred to the PVDF membrane, and the milk was blocked for two hours. The membrane was washed three times with TBST (10 min/time), added with the primary antibody at 4°C overnight, then washed three times with TBST (10 min/time), and the secondary antibody was incubated for two hours. After TBST washing, the membrane was incubated with an ECL high-sensitivity developer and then placed. It was developed in a gel imager.

Apoptosis analysis

Cells (2×10^5) were seeded onto a 6-well plate for each group overnight and then treated with GEM (1 μM) for the indicated time. After incubation, the medium was collected, and the cells were digested with trypsin without EDTA, and incorporated into the previously collected medium. Total cells were collected by centrifugation. Follow the Annexin V-FITC/PI double staining kit, add twice staining reagents in turn, incubate at room temperature for 10 min in the dark, and then perform apoptosis analysis by flow cytometry.

Subcutaneous neoplasia in mice

All animal studies were conducted according to the guidelines provided by the Animal Ethics Committee of Dalian Medical University (Dalian, China). We inoculated SW1990 cells (5×10^6) that induced overexpression of OLA1 into the forelimbs of the Balb/c nude mice aged 4 to 6 weeks and divided the animals into 4 groups (Vector, $OLA1^{iOE}$ group, Vector GEM group, $OLA1^{iOE}$ GEM group), 13 in each group. Seven days after the inoculation, the OLA1-induced overexpression group was given 1 mg / mL Dox 5% sugar water, and the Vector group was assigned 5% control sugar water, which was replaced every two days. The tumor volume was measured every 2-3 days starting on the 8th day of inoculation. It is reported in the literature that the Tet-On overexpression system is fully functional when the animals are fed Dox for about 12 days. To prevent OLA1 overexpression from affecting cell proliferation, the GEM (25 mg/kg) first injection time was determined to be on the 14^{th} day after tumor inoculation, every two days for a total of 7 injections. We inoculated PANC-1-shOLA1 cells and shNC cells (5×10^6) into the forelimb armpits of 5 week-old SCID-NOD mice and divided the animals into six groups (shNC, shOLA1, shNC GEM, shOLA1 GEM, shNC GEM GDC-0449, shOLA1 GEM GDC-0449), when the tumor size is 0.5 cm^3, GEM (25 mg/Kg) is given intraperitoneally every two days, and GDC-0449 or the corresponding solvent is given by gavage every day.

Immunohistochemistry and tissue array

The human cancer tissue specimens were collected by surgical resection after obtaining consent. A tumor (5×3×3 mm) and normal adjacent tissues with a distance of 2-cm from the tumor (3×3×5 mm) were prepared. The detailed clinicopathological data were scored based on the tumor classification of the American Joint Committee on Cancer (AJCC)/International Union Against Cancer (UICC) tumor staging system. The pathological types of paraffin-embedded slides were rechecked by HE staining before immunostaining. Subcutaneous tumor tissues of nude mice were fixed in 4% paraformaldehyde, dehydrated, paraffin-embedded, and cut into 4 μm sections. Next, after transfection of 48 h, cells were fixed in 4% paraformaldehyde. Endogenous peroxidase activity in the tissue sections or fixed cells was blocked with a 3% hydrogen peroxide solution (Sangon Biotech). The antigens were retrieved, and the nonspecific binding was blocked by 4% normal goat serum (Gibco). Subsequently, tissue sections or cell coverslips were incubated with different primary antibodies, followed by HRP conjugated goat anti-rabbit IgG (1:1000, Cell Signaling, MA, USA). Then, 3, 3′diaminobenzidine (DAB) chromogen substrate solution was utilized to visualize the results. For the tissue microarray construction, all cancer specimens were histopathologically re-evaluated and the representative areas were marked. The average score for each slide was obtained by two independent pathologists, who calculated QS by multiplying the intensity score by the percentage of the staining area.

QUANTIFICATION AND STATISTICAL ANALYSIS

Data were presented as mean ± standard deviation (SD). SPSS 23.0 calculated IC_{50} of chemotherapeutics in PDAC cells, and GraphPad Prism 9 carried other statistical results. A two-sided tail non-paired Student's t-test was used to compare differences between the treated and control groups. Survival plots were drawn on Kaplan-Meier analysis, and a log rank test was used to assess statistical significance. Significance was defined as $^*P < 0.05$, $^{**}P < 0.01$, $^{***}P < 0.001$.